

EFFECT OF INTERPLANE CORRELATION ON THE TWO-PLANE MULTITURN INJECTION EFFICIENCY

A. Lauterbach, G. Franchetti^{1,2}, Institute for Applied Physics, Goethe University, Frankfurt, Germany

¹GSI Helmholtzzentrum für Schwerionenforschung GmbH, Darmstadt, Germany

² Helmholtz Research Academy Hesse for FAIR (HFHF), Frankfurt, Germany

Abstract

Beamlets provided by LINACs for injection into ring accelerators are subject to interplane correlation effects. Preliminary studies have shown that these correlations negatively affect the efficiency of one-plane multiturn injection. This study shows the effect of different grades of correlation between the transverse planes of the injected beamlets on the injection efficiency of two-plane multiturn injection at the simulation example of SIS-18.

2-PLANE MULTITURN INJECTION

Within the well-known process of multiturn injection (MTI), which has been subject to many studies in the past [1–3], particle beamlets are accumulated turn by turn to fill the available phase space as well as possible while keeping the overall beam emittance low. This process is also called phase space painting. The parameters to be optimized originate from different aspects of the machine and injection setup, for example the tune of the machine, the beta functions of the machine at the entry point of the beamlets, the injection emittance of the beamlets and many others. The overall goal is to inject as many particles into phase space as possible, obeying Liouville's law and avoiding emittance blow-up. More recently, there have been dedicated studies for two-plane MTI [4, 5]. Two-plane MTI extends this optimization process to both transverse planes, x and y , which enables the vertical transverse phase space to be painted as well. This injection method requires different physical machine configurations, such as a tilted electrostatic septum (ES), to allow the entry of the beam with angles y' different from zero. As for conventional one-plane MTI, the injection scheme is designed with a local orbit bump, which is performed by four steerer magnets each in x and y independently. The decrease in steerer strength is defined separately for the x - and y -plane by decrease functions f_x and f_y which can follow different kinds of curves, for example linear or exponential.

BEAM CORRELATION

The correlation between the x - and y -plane of a beam is described by the second order beam moments matrix or covariance matrix C [6]:

$$C = \begin{pmatrix} \langle xx \rangle & \langle xx' \rangle & \langle xy \rangle & \langle xy' \rangle \\ \langle x'x \rangle & \langle x'x' \rangle & \langle x'y \rangle & \langle x'y' \rangle \\ \langle yx \rangle & \langle yx' \rangle & \langle yy \rangle & \langle yy' \rangle \\ \langle y'x \rangle & \langle y'x' \rangle & \langle y'y \rangle & \langle y'y' \rangle \end{pmatrix}. \quad (1)$$

This matrix provides information on how certain phase space coordinates of the beam are correlated with each other. Generally, all elements of the machine lattice that act on the cross-plane elements of C are potential coupling sources. In the ideal case of a decoupled beamline the cross-plane terms of C are zero, but experimental observations have shown measurable coupling effects originating from the linear accelerator section and/or the transfer channel [6]. In this work, we model the interplane correlations caused by an unidentified coupling element. In practical beamlines, such coupling effects may arise from skew quadrupole fields or imperfections in beamline alignment and optics. To simulate the coupling, we introduce two parameterized 4×4 transformation matrices M_1, M_2 of the form:

$$M_1 = \frac{1}{\sqrt{1 + \kappa^2}} \begin{pmatrix} 1 & 0 & \kappa & 0 \\ 0 & 1 & 0 & \kappa \\ -\kappa & 0 & 1 & 0 \\ 0 & -\kappa & 0 & 1 \end{pmatrix} \quad (2)$$

with $\kappa \in \mathbb{R}$ and

$$M_2 = e^G = \begin{pmatrix} \cos \lambda I & \tilde{\lambda} K \\ -\tilde{\lambda} K & \cos \lambda I \end{pmatrix} \quad (3)$$

with

$$K = \begin{pmatrix} \ell & k \\ k & \ell \end{pmatrix}, \quad G = \begin{pmatrix} 0 & K \\ -K & 0 \end{pmatrix}, \quad \tilde{\lambda} = \frac{\sin \lambda}{\lambda} \quad (4)$$

with $k, \ell, \lambda \in \mathbb{R}$.

The matrix M_1 represents an idealized direct mixing between transverse planes and fulfills the symplectic condition [7], when a pre-factor of $1/\sqrt{1 + \kappa^2}$ is applied, ensuring that the transformation is physically consistent. Matrix M_2 is built from a generator G with $M_2 = e^G$ and corresponds to a symplectic transformation that resembles a smoother rotational coupling in four-dimensional phase space. The parameterized forms of M_1 and M_2 allow changes in the injection efficiency to be traced back to a single coupling parameter while keeping all other simulation parameters constant. Since multi-turn injection is performed via a closed orbit bump, it is crucial to apply the coupling transformation only to the incoming beam, not to the reference closed orbit. To achieve this, the closed orbit coordinates \tilde{X}_{CO} must be explicitly accounted for. While the beam coordinates \tilde{X}

are defined with respect to the nominal beamline center at $(0, 0, 0)^T$, the coupling transformation must be applied relative to the offset from the closed orbit:

$$\vec{X}_{\text{corr}} = \vec{X}_{CO} + M(\vec{X} - \vec{X}_{CO}), \quad (5)$$

where M is a general matrix representing M_1 and M_2 respectively. This ensures that the introduced correlation affects only the injected beam, preserving the integrity of the closed orbit configuration.

Coupling Coefficient

The evolution of the covariance of the beam coordinates can be calculated at each instant of the process by applying Eq. (1). As a measure of the resulting correlation factor of the beam at the end of the injection process, a coefficient T is introduced (adapted from [8]):

$$T = \frac{t}{1+t}, \quad (6)$$

where

$$t = \frac{\sqrt{\langle xx \rangle \langle x'x' \rangle - \langle xx' \rangle^2} \sqrt{\langle yy \rangle \langle y'y' \rangle - \langle yy' \rangle^2}}{\sqrt{\det C}} - 1. \quad (7)$$

Defining T like in Eqs. (6) and (7) ensures normalization to a maximum of 1 for better comparison of the outcome. For a strongly coupled beam $T \rightarrow 1$, whereas in absence of coupling $T = 0$.

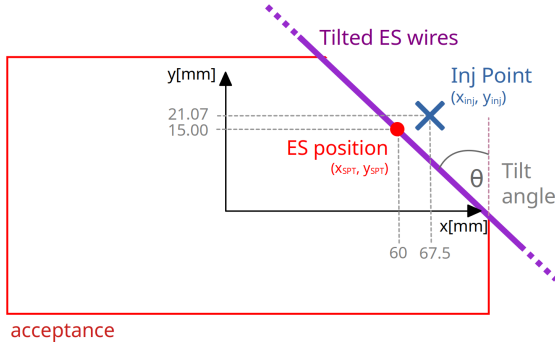


Figure 1: Schematic drawing of the tilted septum geometry and the injection coordinates used for two-plane multiturn injection.

Injection efficiency

The injection efficiency η_{inj} is - for the purpose of this work - defined as $\eta_{\text{inj}} = \frac{N_{p,\text{end}}}{N_{p,\text{inj}}}$ with $N_{p,\text{end}}$ being the number of particles that "survive" the simulation process without getting labeled as "lost" and $N_{p,\text{inj}}$ being the number of particles initialized within the simulation processed, displaying the total number of particles injected.

SIMULATION

For the purpose of this work, a two-plane MTI simulation code was implemented in Fortran 2018, utilizing the

Table 1: Simulation Settings used in this work for SIS18-lattice with U_{28+}^{238} ions

Parameter	Value	Unit	Description
N_b	10^4	[1]	Particles per beamlet
ϵ_x / ϵ_y	5 / 5	[mm-mrad]	Emitance, x/y-plane
Q_x / Q_y	4.238/3.422	[1]	Tune, Two-plane MTI
E_{nuc}	11.4	[MeV/u]	Energy per nucleon
$\alpha_x(s_{\text{Septum}})$	-1.3862	[rad]	Twiss α , x-plane
$\beta_x(s_{\text{Septum}})$	14.919	[m]	Twiss β , x-plane
$\alpha_y(s_{\text{Septum}})$	-0.66484	[rad]	Twiss α , y-plane
$\beta_y(s_{\text{Septum}})$	10.517	[m]	Twiss β , y-plane
θ	45	[deg]	Septum tilt angle

MICROMAP library for beam initialization and tracking. The SIS18 lattice was used as a representative synchrotron lattice. The general simulation settings for all simulation runs can be extracted from Table 1. The code tracks all particles of the beam injected for a certain total number of n turns in the ring. The initialization of particles is performed turn-by-turn, generating a number of particles N_b with a Gaussian distribution cut at 3σ around an injection coordinate $(x_{\text{inj}}, x'_{\text{inj}}, y_{\text{inj}}, y'_{\text{inj}})$. This injection coordinate is defined by the septum position $(x_{\text{SPT}}, y_{\text{SPT}})$ plus an offset in x and y with values shown in Fig. 1 to cover the transverse beam size and avoid scraping particles at the septum right at injection. The coordinates x'_{inj} and y'_{inj} are calculated according to the matching condition $x'(s_{\text{inj}}) = x(s_{\text{inj}})[- \alpha_x(s_{\text{inj}}) / \beta_x(s_{\text{inj}})]$, where $\alpha(s_{\text{inj}})$ and $\beta(s_{\text{inj}})$ are the Twiss parameters at the longitudinal injection location s_{inj} . The calculation is the same for the y -coordinate accordingly. While the injection coordinate stays the same for each beamlet of N_b particles, the decreasing steerer strengths are calculated each turn, enabling phase space painting. In this work, a linear local orbit bump decrease was chosen, implemented using fixed slopes of the form $f_x = x_B(i_t) = x_{B,\text{max}} - m_x i_t$ with $m_x = x_{B,\text{max}}/j$ and $f_y = y_B(i_t) = y_{B,\text{max}} - m_y i_t$ with $m_y = y_{B,\text{max}}/j$ where $m_x = 2.72$ mm and $m_y = 1.00$ mm. Right after injection, the particle data is manipulated by matrix multiplication with M_1 or M_2 respectively, as shown in Eq. (5). The total particle number $N_{p,\text{tot}}$ is tracked at every turn, as well as the phase space coordinates and injection information of each particle, such as an index of particle number and injection turn. The simulation is performed for several values of κ in M_1 , respectively k and l in M_2 . To keep simulations with the Matrix M_2 also as a one-knob-model, the values for k and l are kept constant at $k = l = \lambda / \sqrt{2}$, such that λ remains as the one knob of the model. Simulations are then performed varying the value of κ and λ in ten equidistant steps between 0 and 0.1 and further in steps of 0.05 up to 0.45. The results are listed in Table 2 and shown graphically in Fig. 2.

DISCUSSION

The results are listed in Table 2 and shown graphically in Fig. 2. The simulation results show a decreasing injection efficiency when increasing the correlation strength param-

Table 2: Injection efficiency and coupling coefficient as functions of the correlation strength parameters.

TWO PLANE MTI Correlation Strengths κ, λ [-]	Injection Efficiency η_{inj} [%]		Coupling Coefficient T [-]	
	M_1	M_2	M_1	M_2
	0.00	85.17	85.17	5.90e-4
0.01	84.91	85.80	2.01e-2	1.13e-2
0.02	82.46	85.31	6.73e-2	3.67e-2
0.03	77.11	83.52	0.1345	7.45e-2
0.04	68.98	80.03	0.2126	0.1219
0.05	59.35	74.95	0.2937	0.1755
0.06	50.43	68.46	0.3720	0.2322
0.07	42.86	61.56	0.4442	0.2895
0.08	36.61	54.55	0.5088	0.3456
0.09	31.49	48.38	0.5655	0.3990
0.10	27.05	42.88	0.6148	0.4482
0.15	13.93	24.57	0.7765	0.6403
0.20	0.082	15.15	0.8560	0.7542
0.25	0.052	0.099	0.8987	0.8232
0.30	0.036	0.071	0.9238	0.8658
0.35	0.026	0.055	0.9395	0.8940
0.40	0.020	0.043	0.9499	0.9134
0.45	0.016	0.034	0.9571	0.9273

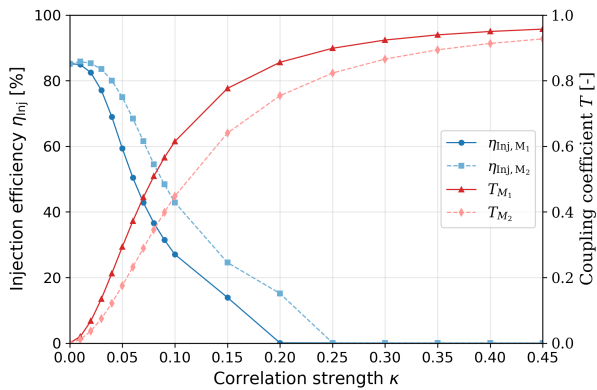


Figure 2: Evolution of the injection efficiency and coupling coefficient as functions of the correlation strengths.

ters κ and λ . As these are the only variables changed within the simulation settings, the resulting decreasing efficiency can be traced back to the change of correlation strength only. It is visible that the effect of the model using M_2 is milder to the efficiency decrease than the model using M_1 . While both procedures, the one using M_1 and the one using M_2 , preserve the total phase-space volume, in comparison to M_1 which induces more of a shear-like coupling, the generator-based matrix M_2 produces a smoother redistribution of the beam in four dimensional phase space, which leads to a weaker decrease of the injection efficiency.

The effect of inter-plane coupling of the incoming beam on the performance of multiturn injection is significantly stronger for two-plane MTI than for one-plane MTI [9]. This behaviour can likely be explained by the exchange of trans-

verse emittance between the horizontal and vertical plane while the total phase space volume is preserved. Since both transverse planes are populated with particles during the process of two-plane MTI, any redistribution of emittance directly influences the injection process resulting in particle losses. One-plane MTI, in contrast, leaves a large part of vertical phase space unoccupied, making it less sensitive to coupling-induced perturbations. This work has been performed for a specific way of applying interplane correlation through the matrices M_1 and M_2 shown in Eqs.(2) and (5). Other variations of coupling matrices may show a comparable effect, as long as they fulfill the symplectic condition.

OUTLOOK

Extending the simulation to include chromaticity, dispersion, and space-charge effects may provide further insights into the beam dynamics of beams injected with existing inter-plane coupling. The application of a non-ideal initial beam distribution would also be an interesting extension of the approach. The extension of the simulation to the simulation of > 1000 turns will give useful insights if and how strong possible after-injection losses occur.

ACKNOWLEDGEMENTS

One of the authors, AL, thanks Oleksiy Dolinskyy and Youssef El-Hayek from GSI for the very useful and constructive discussions on MTI. The authors also thank the members of the accelerator physics group at the Institute of Applied Physics at the Goethe University Frankfurt for valuable discussions.

REFERENCES

- [1] S. Appel and O. Boine-Frankenheim, “Optimization of multi-turn injection into a heavy-ion synchrotron using genetic algorithms”, in *Proc. IPAC2015*, 2015.
[doi:10.18429/JACoW-IPAC2015-THPF007](https://doi.org/10.18429/JACoW-IPAC2015-THPF007)
- [2] Y. E. Hayek, “Minimierung der systemischen anfangsverluste im sis18”, Ph.D. thesis, Goethe University Frankfurt am Main, 2013.
- [3] S. Appel, L. Groening, Y. E. Hayek, M. Maier, and C. Xiao, “Injection optimization through generation of flat ion beams”, *Nuclear Instruments and Methods in Physics Research Section A*, vol. 866, pp. 36–39, 2017.
[doi:10.1016/j.nima.2017.05.041](https://doi.org/10.1016/j.nima.2017.05.041)
- [4] O. Dolinskyy, Y. E. Hayek, D. Ondreka, and P. Spiller, “Enhancing beam intensity in SIS18 by a two-plane multi-turn injection approach”, in *Proc. IPAC'25*, Taipei, Taiwan, pp. 836–839, Nov. 2025.
[doi:10.18429/JACoW-IPAC2025-MOPS141](https://doi.org/10.18429/JACoW-IPAC2025-MOPS141)
- [5] S. Zhang *et al.*, “Simulation and parameter optimization of 6-dimensional phase space injection scheme based on hiaf-bring”, *Nuclear Instruments and Methods in Physics Research Section A*, vol. 1064, 2024.
[doi:10.1016/j.nima.2024.169348](https://doi.org/10.1016/j.nima.2024.169348)

- [6] M. T. Maier, A. Bechtold, L. Groening, J. M. Maus, and C. Xiao, “Rose - a rotating 4d emittance scanner”, in *Proc. IBIC2019*, pp. 669–673, 2019.
[doi:10.18429/JACoW-IBIC2019-THA003](https://doi.org/10.18429/JACoW-IBIC2019-THA003)
- [7] D. Edwards and L. Teng, “Parametrization of linear coupled motion in periodic systems”, *IEEE Transactions on Nuclear Science*, pp. 885–888, Jul. 1973.
[doi:10.1109/TNS.1973.4327279](https://doi.org/10.1109/TNS.1973.4327279)
- [8] C. Xiao *et al.*, “Measurement of the transverse four-dimensional beam rms-emittance of an intense uranium beam at 11.4 mev/u”, *Nuclear Instruments and Methods in Physics Research Section A*, vol. 820, pp. 14–22, 2016.
[doi:10.1016/j.nima.2016.02.090](https://doi.org/10.1016/j.nima.2016.02.090)
- [9] A. Lauterbach and G. Franchetti, “Effects of beam plane correlation on injection efficiency”, in *Proc. IPAC'25*, Taipei, Taiwan, pp. 999–1001, Nov. 2025.
[doi:10.18429/JACoW-IPAC2025-TUPB021](https://doi.org/10.18429/JACoW-IPAC2025-TUPB021)